

SURFACE STRUCTURE OF TETRAHEDRAL-COORDINATED AMORPHOUS  
DIAMOND-LIKE CARBON FILMS GROWN BY PULSED LASER DEPOSITION

Conf-941144--166

T. W. MERCER\*, N. J. DiNARDO\*\*, L. J. MARTINEZ-MIRANDA\*\*\*, F. FANG\*\*\*\*, T. A. FRIEDMANN\*\*\*\*\*, J. P. SULLIVAN\*\*\*\*\*, AND M. P. SIEGAL\*\*\*\*\*

\* Drexel University, Department of Physics and Atmospheric Science, Philadelphia, PA 19104

\*\* University of Pennsylvania, Department of Materials Science and Engineering, Philadelphia, PA 19104

\*\*\* Kent State University, Department of Physics, Kent, OH 44242 and University of Maryland, Department of Materials and Nuclear Engineering, College Park, MD 20742

\*\*\*\* University of Pennsylvania, Department of Electrical Engineering, Philadelphia, PA 19104

\*\*\*\*\* Sandia National Laboratories, Albuquerque, NM 87185-0345

**ABSTRACT**

The structure and composition of tetrahedral-coordinated amorphous diamond-like carbon films (a-tC) grown by pulsed laser deposition (PLD) of graphite has been studied with atomic force microscopy (AFM). The nanometer-scale surface structure has been studied as a function of growth parameters (e.g., laser energy density and film thickness) using contact-mode and tapping-mode AFM. Although the surfaces were found to be generally smooth, they exhibited reproducible structural features on several size scales which correlate with the variation of laser energy and the effects of excited ion etching.

Introduction

Due to significant developments in the area of high powered ultra-violet (UV) excimer lasers, the technique of pulsed laser deposition (PLD) has become a very effective means for depositing high-quality hydrogen-free tetrahedral-coordinated amorphous diamond-like carbon (a-tC) films. A critical factor for deposition is the creation of a high flux beam of energetic carbon ions in the fractional keV range. In this study, we have examined the surfaces of several films grown by PLD at a variety of laser energy densities. These films are grown by ablation of a graphite target with a KrF (248 nm) pulsed excimer laser. Films approximately 1400 Å thick were grown on commercial grade Si(100) wafers at three different laser energy densities of 46 J/cm<sup>2</sup>, 27 J/cm<sup>2</sup> and 11 J/cm<sup>2</sup>

Experiment

The PLD process is described elsewhere.<sup>1</sup> After a-tC deposition, the samples were oxygen plasma etched for a period of 360 seconds in order to remove graphitic carbon.<sup>2</sup> This procedure was performed in a Denton Model PE-120 plasma chamber

## **DISCLAIMER**

This report was prepared as an account of work sponsored by an agency of the United States Government. Neither the United States Government nor any agency thereof, nor any of their employees, make any warranty, express or implied, or assumes any legal liability or responsibility for the accuracy, completeness, or usefulness of any information, apparatus, product, or process disclosed, or represents that its use would not infringe privately owned rights. Reference herein to any specific commercial product, process, or service by trade name, trademark, manufacturer, or otherwise does not necessarily constitute or imply its endorsement, recommendation, or favoring by the United States Government or any agency thereof. The views and opinions of authors expressed herein do not necessarily state or reflect those of the United States Government or any agency thereof.

## **DISCLAIMER**

**Portions of this document may be illegible in electronic image products. Images are produced from the best available original document.**

with an oxygen pressure of  $400 \pm 20$  mTorr and an RF power of 50 W. The set of samples under study were etched simultaneously to assure identical etching conditions. After etching, the samples were imaged with a Digital Instruments Nanoscope III atomic force microscope (AFM). When the AFM was operated in the contact mode, it was found that the  $\text{SiN}_3$  tips were susceptible to a significant amount of damage inhibiting the ability to obtain images with acceptable spatial resolution. This occurs because of rapid tip wear due to the extreme hardness of these surfaces. In order to avoid this problem, tapping mode (intermittent-contact imaging) was utilized to improve image quality.

Before etching, the surfaces of the a-tC films were found to be remarkably flat with height variations on the order of 1 nm over a 500 nm x 500 nm image. For a comparison of roughness, a surface plot with a 45° pitch has been added to each figure. Figures 1, 2 and 3 are AFM images obtained after etching the surfaces of the samples grown with laser energy densities of 46 J/cm<sup>2</sup>, 27 J/cm<sup>2</sup>, and 11 J/cm<sup>2</sup>, respectively. Nanoscale clusters with sizes and shapes depending on the laser energy density are clearly seen. The cluster size decreases with increasing laser energy density in going from a laser energy density of 27 J/cm<sup>2</sup> to 46 J/cm<sup>2</sup>; this trend is less apparent for samples grown with energy densities increasing from 11 J/cm<sup>2</sup> to 27 J/cm<sup>2</sup>. Increases in roughness were also apparent as the energy densities were increased.

## Discussion

The formation and transport of the laser-induced plasma are key factors in the generation of high velocity ions.<sup>3</sup> We begin with a brief discussion on how these two key factors are affected by the laser energy density. From the outset of the graphite target ablation, an extremely fast free expansion of the plasma allows carbon atoms to maintain their ionic state. The expansion serves to lower the concentration of carbon ions and electrons to such a degree so as to inhibit significant recombination.<sup>4,5</sup> The acceleration of the ions or transport of the plasma occurs in two phases.<sup>6</sup> The first phase occurs in a region from the target to a distance approximately equal to the radius of the focused beam. In this region ions are ejected directly normal to the surface of the target in a manner similar to electron- or ion-stimulated desorption. At the boundary between the first and second phases, the laser pulse is absorbed by inverse bremsstrahlung. The second phase occurs due to the immense heat generated which causes the plasma to expand spherically about the laser spot center. Near the boundary between phase the two phases, the velocities of the ions are approximately equal to the local velocity of sound. At the end of the second phase, the ion velocities can approach hypersonic speeds. The total energy density not only affects the free expansion of the initial plasma formation and therefore the charge state of the ionized carbon present, but also the transport of the plasma and thus the final kinetic energy. A theory has been developed by Stevefelt and Collins<sup>7</sup> in which they considered the case of carbon ablation with a Q-switched Nd-YAG laser. For a given focused intensity,  $\Phi_0$  [W/cm<sup>2</sup>], they showed that the resulting ion energy is equal to:

$$E = 330 \left( \frac{\Phi_0}{10^{10} \text{ W cm}^{-2}} \right)^{4/9} \text{ (eV)} \quad (1)$$

The dominant ions were predicted to be  $C^{3+}$  and  $C^{4+}$  over a wide range of input intensities.

For the a-tC film surfaces investigated in this study, a clear relationship exists between the roughness of the plasma-etched surfaces and the laser energy density used for ablation of the graphite target. Changes in the sizes and shapes of the nanoscale clusters are also apparent between  $46 \text{ J/cm}^2$  and  $27 \text{ J/cm}^2$  but not as evident between  $27 \text{ J/cm}^2$  and  $11 \text{ J/cm}^2$ . It has been suggested that oxygen plasma etching exhibits an accelerated etching rate in areas with dangling bonds.<sup>8</sup> It is quite possible the morphological variations observed in these images are due to the formation of clusters with dangling bond densities inversely proportional to the laser energy density. In this regard, samples grown with a high laser energy density exhibit clusters with a lower density of unpaired electrons. This would also coincide with the variation in roughness as a function of energy density.

### Conclusions

We have shown that, after plasma etching, the films exhibit different cluster sizes and degrees of surface roughness that depend on the laser energy density of the PLD process. In particular, the cluster size appears to increase with decreasing laser energy density while surface roughness decreases with decreasing laser energy. We suspect these effects occur due to the correlation between the kinetic energy of the depositing ions and the laser energy density used in the ablation process.

### Acknowledgments

This work was performed in part at Sandia National Laboratories, Albuquerque, NM and supported by the US DOE under contract DE-ACO4-94AL85000. NJD acknowledges support from the NSF under grant DMR 93-13047. The Scanning Probe Microscopy MRL Central Facility at the University of Pennsylvania is supported by the NSF under grant DMR 91-20668.

### References

1. M. P. Siegal, T. A. Friedmann, S. R. Kurtz, D. R. Tallant, R. L. Simpson, F. Dominguez and K. F. McCarty, in *Mater. Res. Soc. Proc.* (Materials Research Society, San Francisco, 1994), pp. 507.
2. G. S. Sandhu and W. K. Chu, *Appl. Phys. Lett.* **55**, 437 (1989).
3. Carl. B. Collins and Farzin Davanloo, in *Pulsed Laser Deposition of Thin Films* D. B. Chrisey, G. K. Hubler, Eds. (John Wiley and Sons, Inc., New York, 1994), pp. 417.
4. R. R. Goforth and P. Hammerling, *J. Appl. Phys.* **47**, 3918 (1976).
5. M. K. Matzen and J. S. Pearlman, *Phys. Fluid* **22**, 449 (1979).
6. J. Puell, *Z. Nat. Forsch.* **A25**, 1807 (1970).
7. J. Stevefelt and C. B. Collins, *J. Phys. D: Appl. Phys.* **24**, 2149 (1991).
8. Ichiro Watanabe, Katsuhiko Hurata and Yoshikazu Shimamura, *Jpn. J. Appl. Phys.* **33**, 2035 (1994).

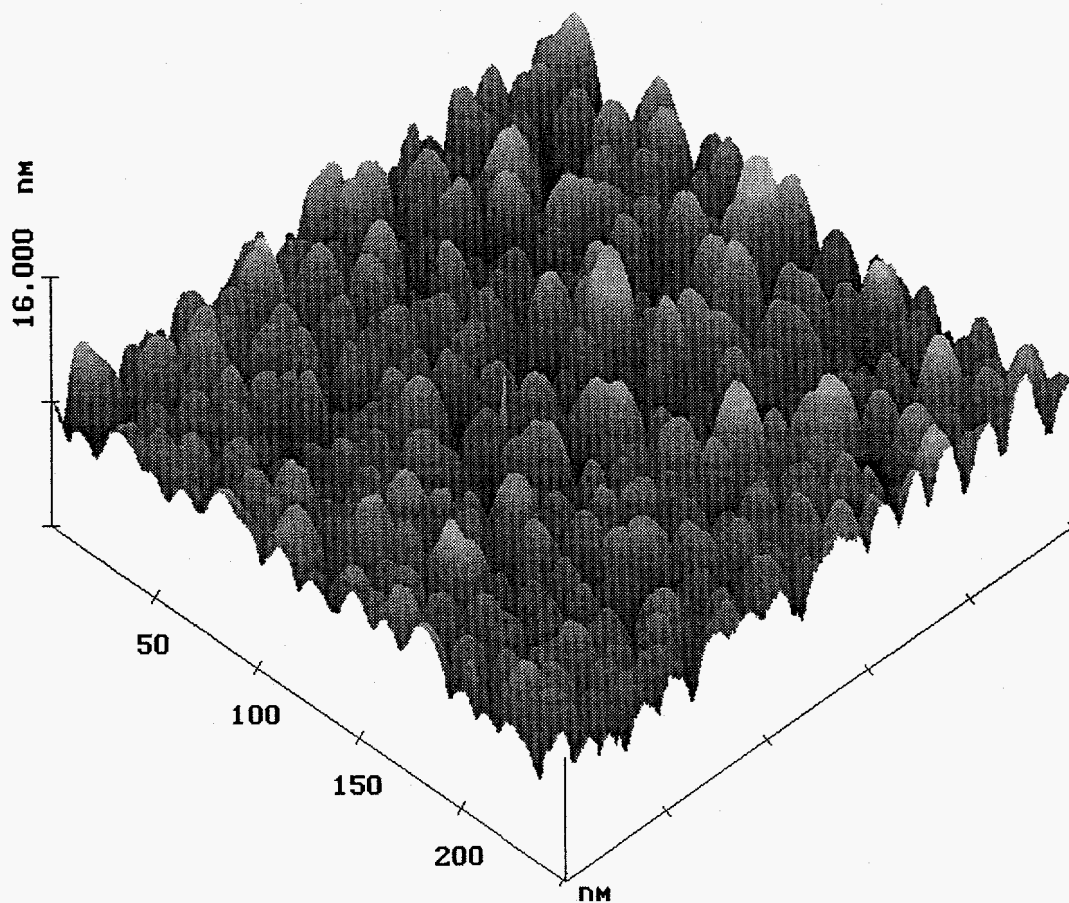
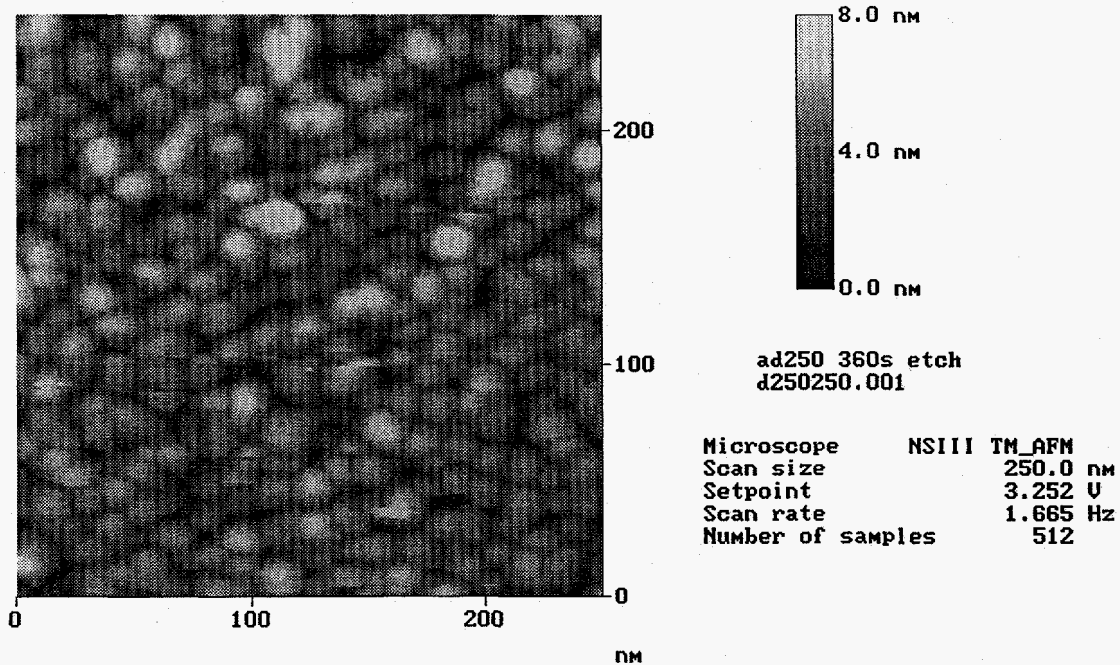


Figure 1 A 500nm X 500 nm AFM image of a sample grown with a laser energy density of  $46\text{J}/\text{cm}^2$ . The above image is a normal "top view" whereas the bottom is a 45 pitch "surface plot".

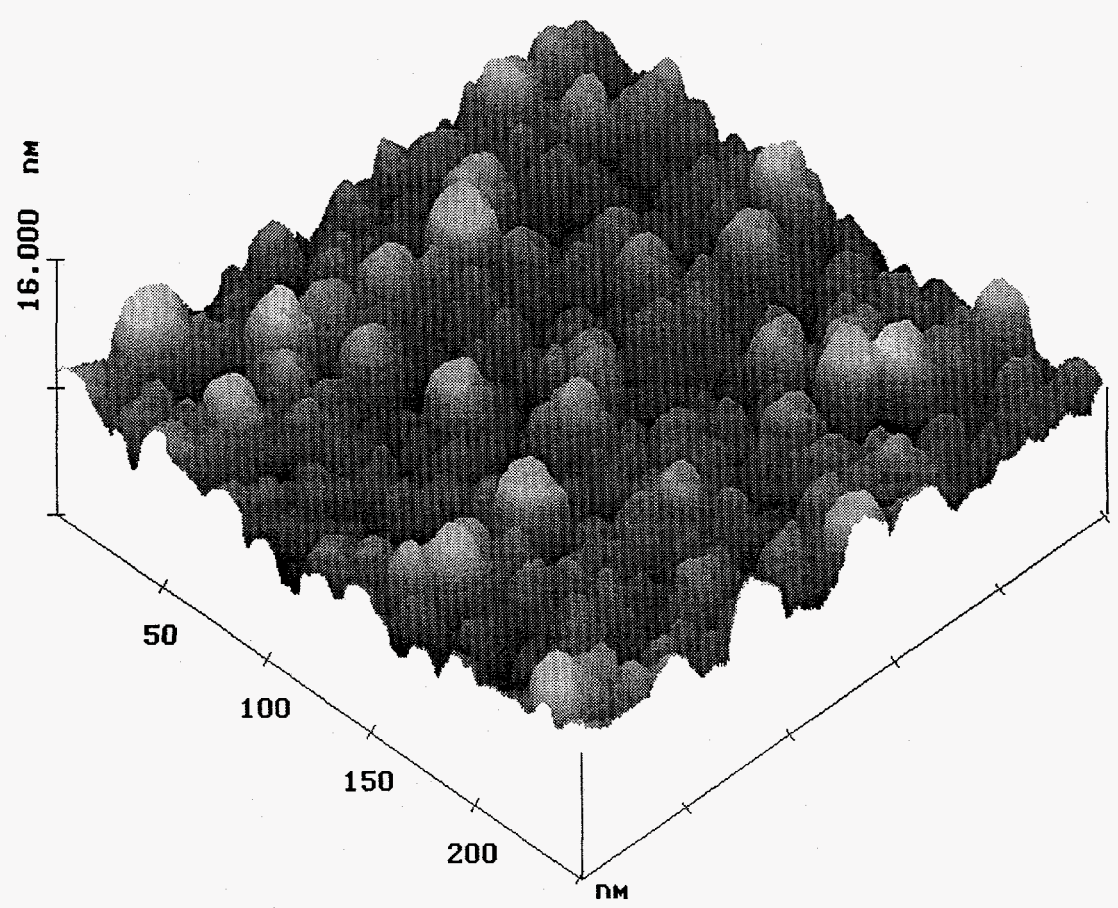
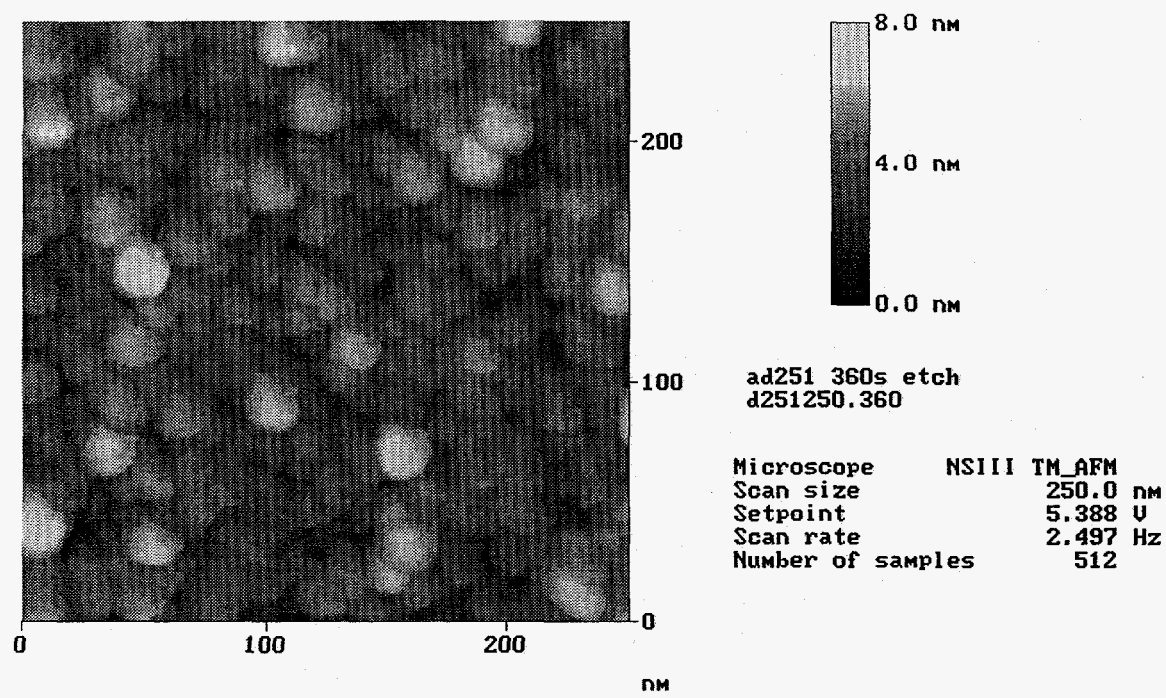


Figure 2 A 500nm X 500 nm AFM image of a sample grown with a laser energy density of 27J/cm<sup>2</sup>. The above image is a normal "top view" whereas the bottom is a 45 pitch "surface plot".

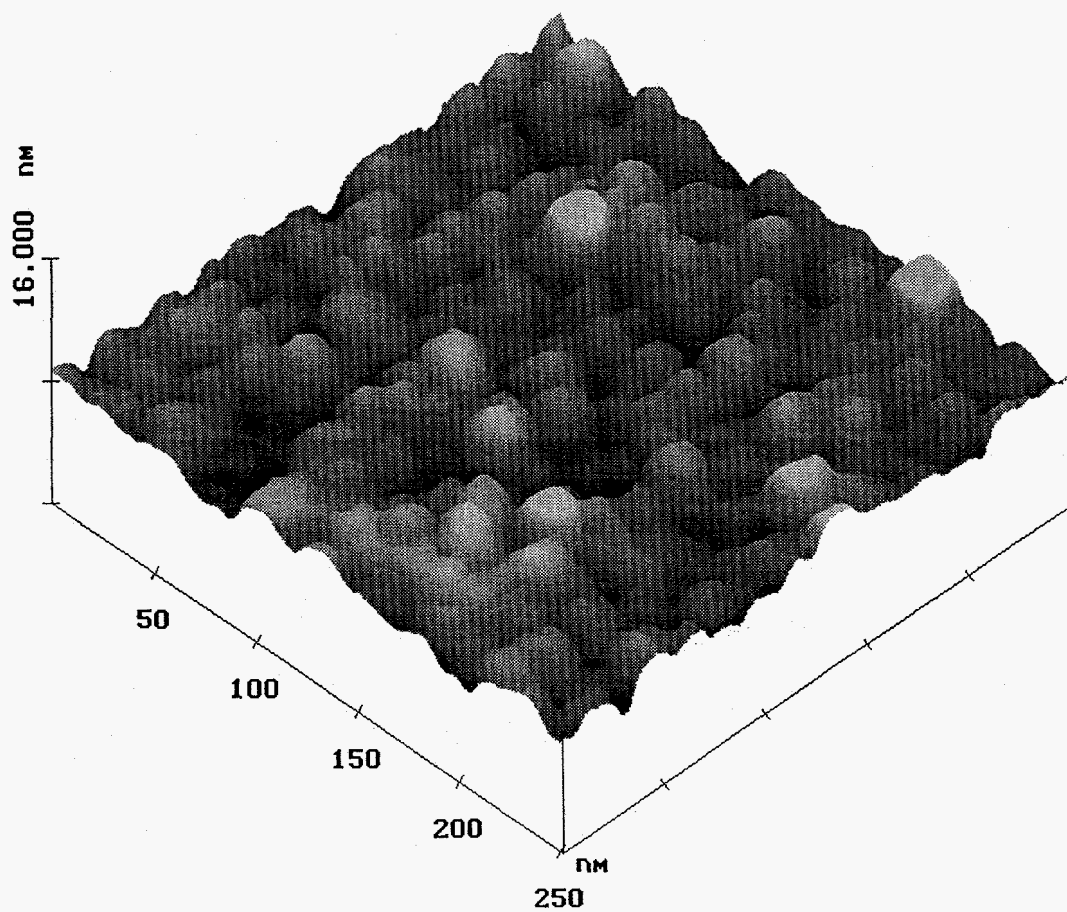
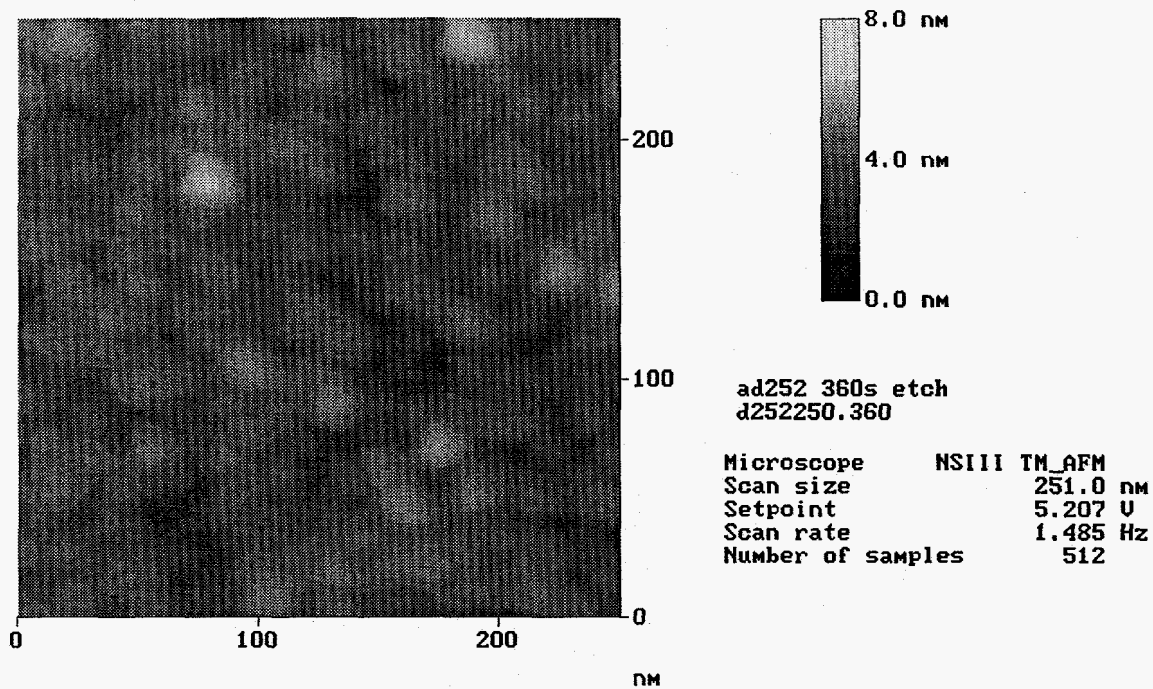


Figure 3 A 500nm X 500 nm AFM image of a sample grown with a laser energy density of  $11\text{J}/\text{cm}^2$ . The above image is a normal "top view" whereas the bottom is a 45 pitch "surface plot".



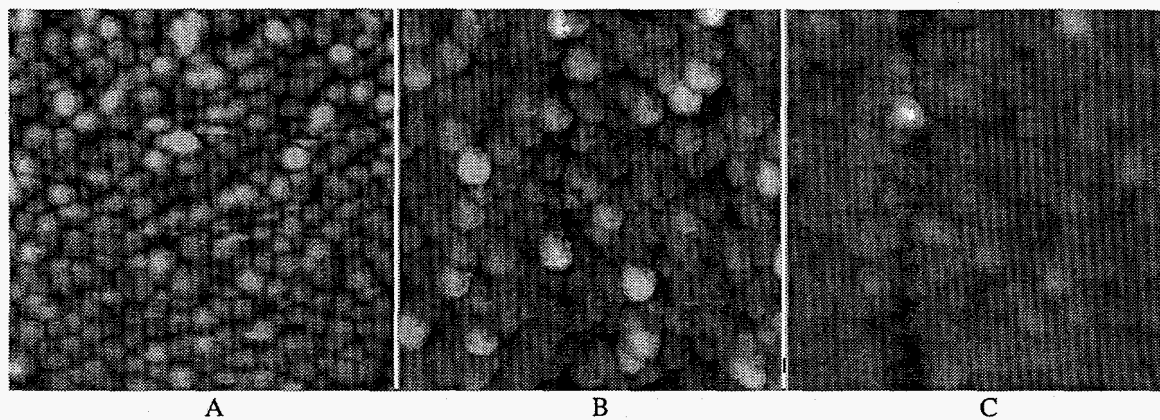


Figure 4 A side by side display of AFM images obtained on samples grown with laser energy densities of (A)  $46 \text{ J/cm}^2$  (B)  $27 \text{ J/cm}^2$  (C)  $11 \text{ J/cm}^2$